Halo and Bunch Purity Monitoring

= Very High Dynamic Beam Profile Measurements; Transversal and Longitudinal

Kay Wittenburg, DESY, MDI

Kay.Wittenburg@desy.de

Outline

- Halo diagnostic:
  - What is Halo?
  - Halo Quantification
- Transversal Halo Measurements with:
  - IPM (**I**onization Beam **P**rofile **M**onitor)
  - LPM (**L**uminescence Beam **P**rofile **M**onitor)
  - Laser
  - Wire Scanners and Scrapers (slow)
  - Optical Methods (fast)
- Longitudinal Halo
  - Bunch Purity
  - "Beam in Gap"
  - Coasting Beam

Monitors have not enough dynamic range.
Slides can be found after the last slide of talk

Outline

- Halo diagnostic:
  - **What is Halo?**
  - Halo Quantification
- Transversal Halo Measurements with:
  - Wire Scanners and Scrapers (slow)
  - Optical Methods (fast)
- Longitudinal Halo
  - Bunch Purity,
  - "Beam in Gap"
  - Coasting Beam

What's Halo?

… because of the beam distribution's phase-space rotations, the observed halo in 1D oscillates, so that halo at different locations along the beam line is observable in differing degrees. For example, at some locations the halo may project strongly along the spatial coordinate and only weakly along the momentum coordinate, while at others the reverse is true, and the halo can be hidden in the spatial projection. In most circumstances, the beam halo from simulation appears as an irreversible effect, when observed in the 2D phase-space distributions. Therefore, it is also important to search for another definition of halo in the 2D phase-space distributions….

-

…it became clear that even at this workshop (HALO 03) **a general definition of "Beam Halo" could not be given,** because of the **very different requirements** in different machines, and because of the **differing perspectives** of instrumentation specialists and accelerator physicists.

From the diagnostics point of view, one thing is certainly clear – by definition halo is low density and therefore difficult to measure…

What is Halo?

From the diagnostics point of view, one thing is certainly clear – by definition halo is low density and therefore difficult to measure…

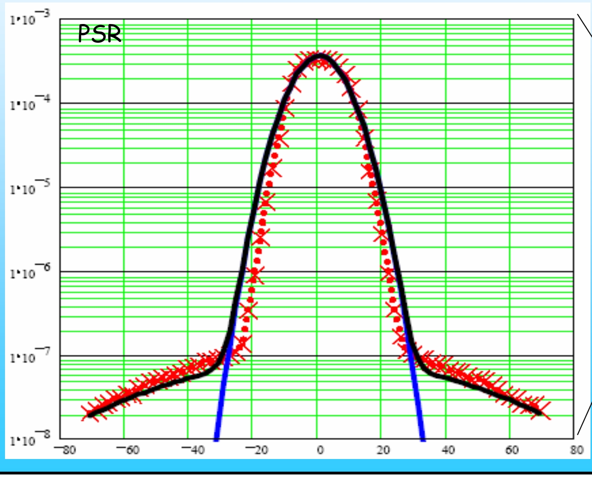

Halo measurements require **high dynamic range instruments** and methods

Dynamic range > 10^5

What is Halo?

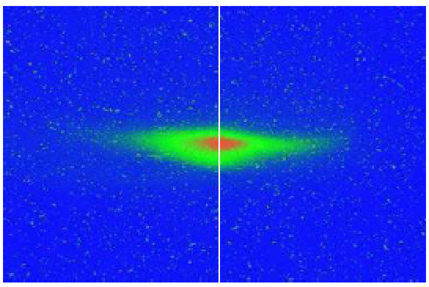

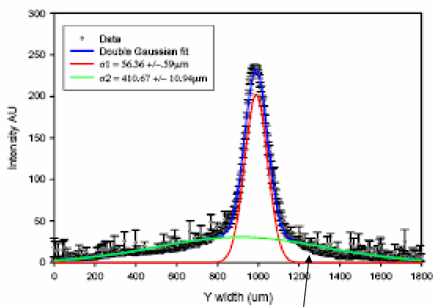

That's not a halo, that's a tail!
Dynamic range <10^3

What is Halo?

•**Sources of halo are:**
- space charge
- mismatch
- beam beam forces
- instabilities and resonances
- RF noise
- Scattering (inside beam, residual gas, macroparticles, photons, obstacles (stripping foil, screens), …)
- nonlinear forces
- misalignments
- electron cloudes
- etc.

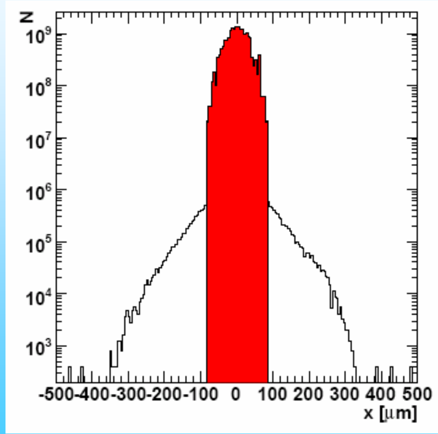

Calculated transverse beam halo
at the ILC-BDS entrance

What is Halo?

- In storage synchrotrons, **background** due to halo can mask the **rare physics processes** and the experiment detectors are often the most **radiation sensitive components** in the accelerator. The beam loss threshold imposed by the most sensitive of the several experiments is often far below that imposed by activation of machine components.
- A number of < 0.1‰ lost particles /bunch appears sometimes to be already critical (e.g. can cause harmful beam loss). We therefore require a beam monitor capable of measuring the transverse beam halo better than this. **The required dynamic range is therefore of the order of 10^5 or better**.

- **Profile measurements are often questioned at the level of a few percent**, the difficulty is easily seen in making halo measurements already at the level of 10^{-4} and beyond.

Outline

- Halo diagnostic:
  - What is Halo?
  - **Halo Quantification**
- Transversal Halo Measurements with:
  - Wire Scanners and Scrapers (slow)
  - Optical Methods (fast)
- Longitudinal Halo
  - Bunch Purity,
  - "Beam in Gap"
  - Coasting Beam

HALO QUANTIFICATION

It is important to have a definition of halo in 1D spatial projections for which experimental measurements are relatively easy to obtain.

However, because of the beam's phase-space rotations, the observed halo in 1D projections oscillates. For example, at some locations the halo may project strongly along the **spatial coordinate** and only weakly along the **momentum coordinate**, while at others the reverse is true, and the halo can be hidden from the spatial projection. Therefore one should extend the 1D work to obtain a halo parameter suitable for description of beam halo in **whole phase space**. This lead naturally to the *kinematic invariants* and are the consequence of the linear forces and symplectic structure imposed by **Hamilton's equations**.

Used mainly in simulations

The excursions above the Gaussian level indicate a large halo.

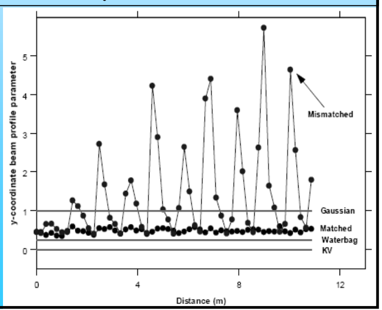

HALO QUANTIFICATION

- There is **no clearly defined separation** between the halo and the main core of the beam. Consequently, there has been some difficulty identifying a suitable quantitative measure of the halo content of a beam in a model-independent way.
- A general characteristic of beam halo is the increased population of the outer part of the beam.
- **Methods have been developed, and computationally studied, to characterize beam halo.**

1) **Kurtosis**
2) **The Gaussian area ratio method**
3) **Ratio of beam core to offset**

Note that a measurement always contains instrumental effects!!!!
True for all methods!

HALO QUANTIFICATION

1) Kurtosis

This method is based on analyzing the **fourth moment of the beam profile**. The kurtosis is a measure of **whether a data set is peaked or flat relative to a normal (Gaussian) distribution**.

$$k \equiv \frac{\left\langle (x-x_0)^4 \right\rangle}{\left\langle (x-x_0)^2 \right\rangle^2} - 2$$

Distributions with high kurtosis have sharp peaks near the mean that come down rapidly to heavy tails. An important feature of such quantifiers is that they are **model independent** and rely only on the characteristics of the beam distribution itself.

Might be not so well suited for us instrumental specialists.

HALO QUANTIFICATION

2) The Gaussian area ratio method:

Unlike the Kurtosis method, this method is not as sensitive to outlying particles but was found to be more useful for experimental data. The Gaussian area ratio method attempts to quantify the "non-Gaussian" component of the beam profile. After the data is filtered, it is fitted to a Gaussian of the form:

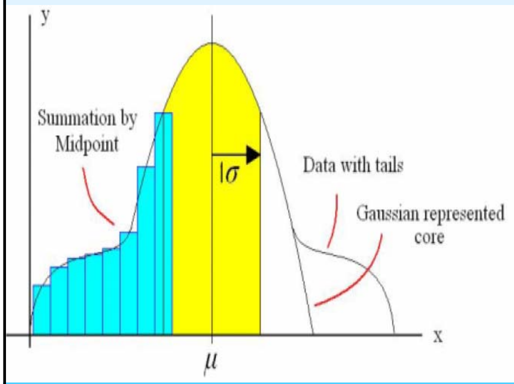

$f(x) = A \exp(-(x-x_0)2/(2\sigma^2))$

In order to represent the core, a Gaussian fit is performed on the top (90 percent) of the profile since most profiles greatly resemble Gaussian's in this region of the beam core. Dividing the total area by the area under the Gaussian outside 1 σ gives a ratio of the tails to the core and, therefore, a quantitative measure of the halo present.

HALO QUANTIFICATION

3) Ratio of beam core to offset:

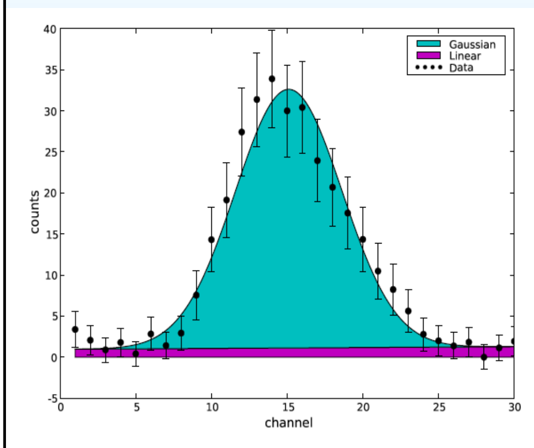

Fit the raw data to the function:
$f(x) = g(x) + l(x)$;
where
$g(x) = N \exp -(x - xo)^2/(2\sigma^2)$
and
$l(x) = c_0 + c_1 x$
The two components of f(x) can be thought of as the Gaussian core g(x) and non-Gaussian tails l(x) of the beam distribution. Defining
$L = \int_{detector} l(x)dx$
and
$G = \int_{detector} g(x)dx$
we can now characterize the beam shape by the ratio L/G. A perfectly Gaussian beam will have L/G = 0, whereas a beam with halo will have L/G > 0.

HALO QUANTIFICATION

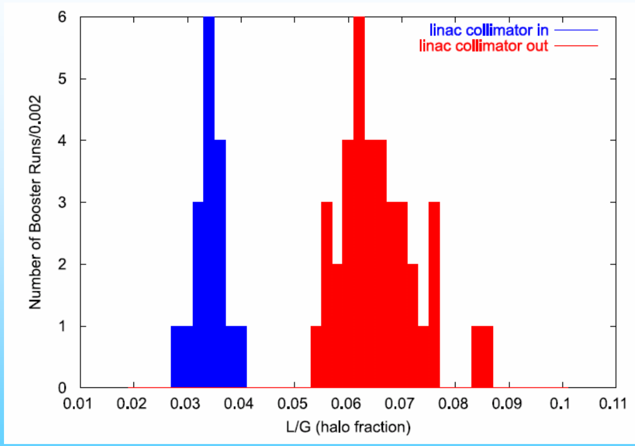

Distribution of L/G values in the Fermilab Booster with and without the linac collimators. (Measured with an IPM)

Outline

- Halo diagnostic:
  - What is Halo?
  - Halo Quantification
- Transversal Halo Measurements with:
  - **Wire Scanners and Scrapers (slow)**
  - Optical Methods (fast)
- Longitudinal Halo
  - Bunch Purity,
  - "Beam in Gap"
  - Coasting Beam

Halo Measurements

- The focus of the **accelerator physicists** is on designing and operating their machines to minimize this halo.
- The focus of the **collimation experts** is on cleanly and efficiently disposing of this halo as it appears, a consequence of the clean and efficient disposal being that useful diagnostic information is often lost, buried in the collimators.
- The focus of the **instrumentation specialists** is twofold;
  - ✓ to provide information useful to the accelerator physicists in their machine tuning efforts to avoid halo formation, and
  - ✓ to provide direct measurement of halo.

This lesson

Definition of halo diagnostics: Classification into three categories.

1. Devices that directly measure halo and halo evolution, and the prime example is the wire scanner.
2. Devices that contribute to the diagnosis of machine conditions that cause halo formation, and an example would be a tune measurement system.
3. Devices that measure the effects of halo development, and an example would be the loss monitor system.

Transversal Halo Measurements

Transversal Halo Measurements with:
- **Wire Scanners and Scrapers (slow)**
- **Optical Methods (fast)**

For
- IPM (**I**onization Beam **P**rofile **M**onitor)
- LPM (**L**uminescence Beam **P**rofile **M**onitor)
- Laser

see slides after the end.

Their dynamic range end at about 10^3!

Wire Scanners and Scrapers

- Used around the world, focus here:
  Dynamic range and sensitivity
- Problems are well known:
  Emittance blow up, wire heating.
- Readout by Scintillators and/or SEM
- Huge dynamic range by:
  - Log-amplifier (PSR)
  - Wire + Scrapers (LEDA)
  - scanning + counting (J-Lab, DESY, AGS)
  - Scraping with collimators (LEP)
  - Other methods
- **Real Halo Measurements**

Wire Scanners at LEDA

(Proton LINAC, SEM readout)

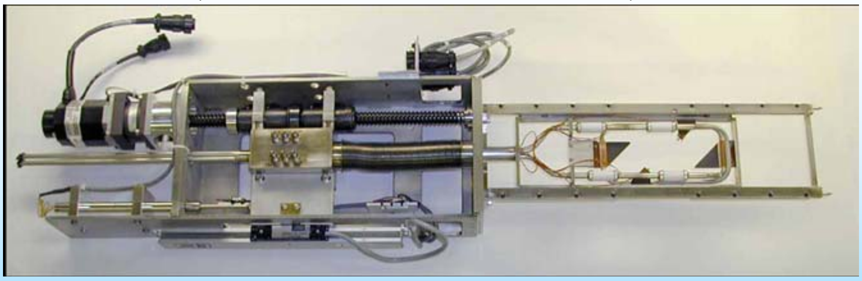

WS can move a 33-μm carbon mono filament and two halo scraper consisting of two graphite scraping devices (one for each side of the distribution).
The high-heat flux testing performed on the prototype scrapers revealed that the design can withstand the thermally induced fatigue loading. The peak heat flux that these scrapers have experienced in actual service is approximately 600 kW/cm^2

Wire Scanners

To plot the complete beam distribution for each axis, the **wire scanner and two scraper data sets must be joined**. To accomplish this joining, several analysis tasks are performed on the wire and scraper data including:

1. Scraper data are spatially differentiated and averaged,
2. Wire and scraper data are acquired with sufficient spatial overlap (where the wire scanner signal rises above the noise),
3. Differentiated scraper data are normalized to the wire beam core data,
4. Normalize data to axis (simple if on same fork)
5. Normalize data to beam current and beam position (true for all kind of halo measurements)!!!!

Before scan: define safe scraper insertion limits (avoid too much heat load) by wire scan data. In SEM mode avoid thermal electron emission!

Procedure explained in:

ANALYSIS OF DATA FROM THE LEDA WIRE SCANNER/HALO SCRAPER*
J. H. Kamperschroer,† General Atomics, Los Alamos,
J. F. O'Hara, Honeywell, L. A. Day, J. D. Gilpatrick, and D. M. Kerstiens, Los Alamos National Laboratory
PAC2001

Wire Scanners

To 1: **Scraper data are spatially differentiated and averaged**

As the scraper marches inward, it intercepts an ever increasing segment of the beam. It is therefore necessary to **differentiate the scraper signal** to determine the transverse distribution. Take scraper data with N-times finer steps than used for the wire scan. This finer stepping allows the **differentiation algorithm to smooth the data**. The numerical derivative can be computed as the difference between two N-point averages on either side of the point in question divided by the spatial separation between them. Larger values of N improve the signal-to-noise ratio, but at the cost of additional time to complete the scrapes.

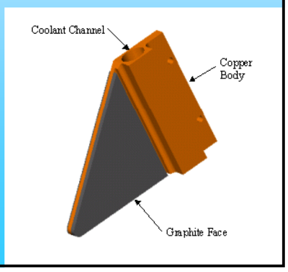

Wire Scanners

to 2: **<u>Wire and scraper data are acquired with sufficient spatial overlap</u>**
The first step in joining the scraper data to the wire scanner data is determining where the data sets overlap. The overlap region consists of wire scanner locations ranging from where the wire scanner signal-to-noise ratio is greater than 2 to the maximum insertion location of the scraper.

to 3 and 4: **<u>Differentiated scraper data are normalized to the wire beam core data and</u>**
<u>Normalize data to axis</u>
Once the region of overlap has been determined, the scraper data must be normalized to attach it to the wire scanner data. The scaling factor is the average of wire scanner to halo scraper signal ratios at two of the three most-inboard points in the overlap region (the most inboard point is excluded). Once scaled, the entire scraper data set is thinned by keeping only every N^{th} scraper point and attached at the connecting points.
Measurements of <u>wire to scraper distances</u> were carried out in Lab. with an uncertainty of 0.25 mm. This implies a positional attachment uncertainty of 0.25 mm. At this point, the resulting three distributions have been combined into a single distribution with uniform step size.

Wire Scanners **<u>and others</u>**

to 5: **<u>Normalize data to beam current and beam position</u>**
Each data point has to be normalized to the measured **<u>beam current and beam position</u>** for each measurement.

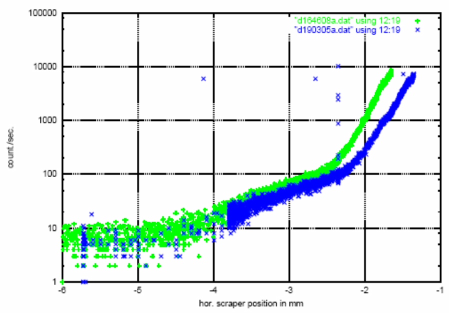

Beam loss rates versus scraper position, black: first measurement, grey: second measurement. During the second measurement the orbit moved about 0.30 mm in 4721 s.

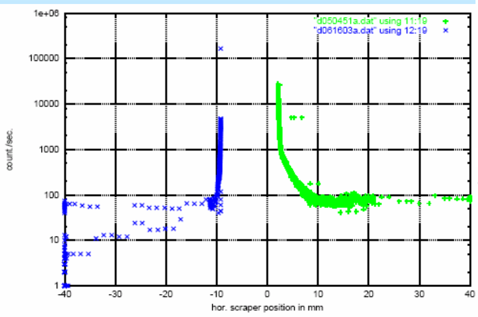

Beam loss rates versus scraper position. The orbit movement causes an artificial asymmetry in the measurement results

Y-axis wire scan

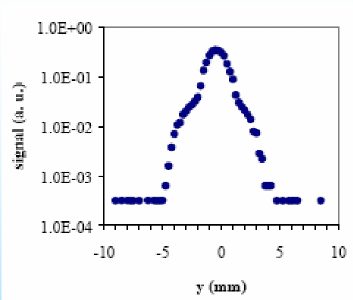

=>

Combined distribution in y.

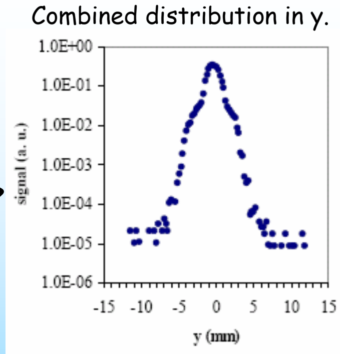

+ +

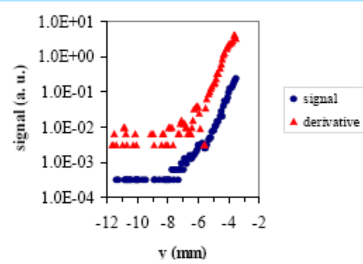

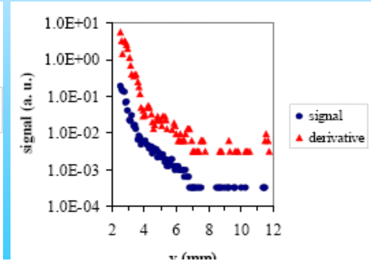

-Y and + Y scrape signal and derivative. The derivative has been multiplied by ten.

Wire Scanners at PSR

linear amplification and 10^5 dynamic range
=> 16-bit D/A converter

As an alternative solution is to process the integrated signal using a logarithmic amplifier. The log amplifier allows the use of standard 12-bit A/D converters.

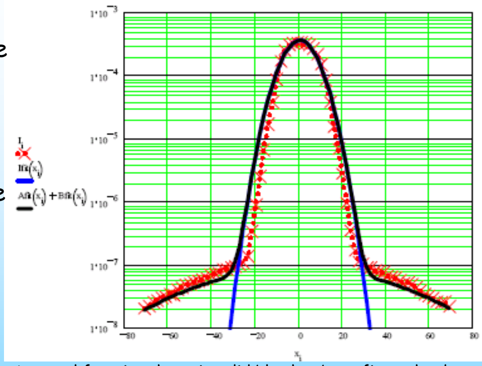

A normal function shown in solid blue has been fit to the data (red x's). A sum of two normal functions is shown in solid black. The x-axis is scaled as scanner position in mm's and the y-axis is log-amp input current in Amps.

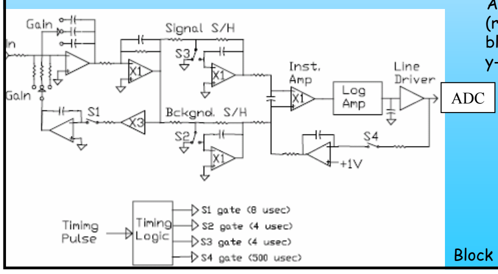

Block diagram of amplifier

Wire Scanners

SEM (LEDA, PSR)

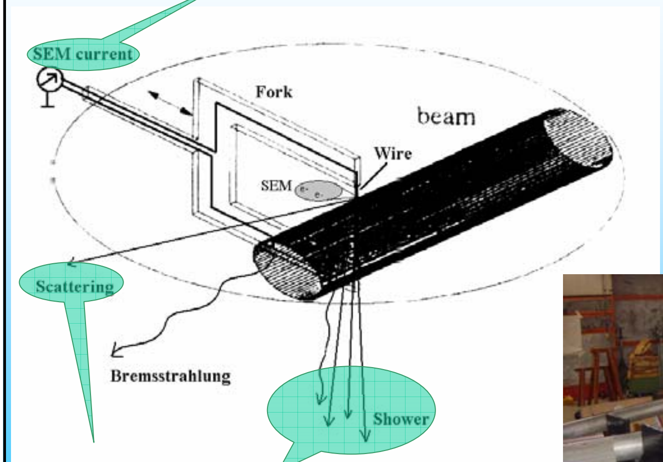

Counting mode, bunch by bunch

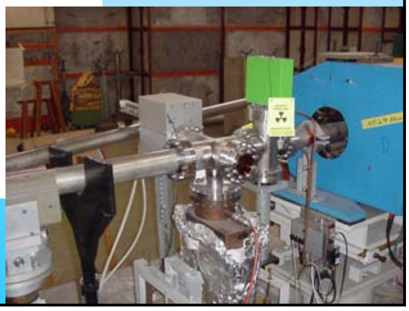

Wire Scanners

Telescope Operation at the extracted beams (AGS)

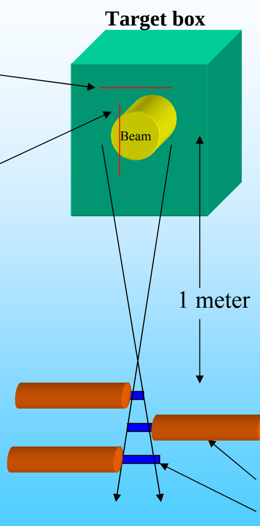

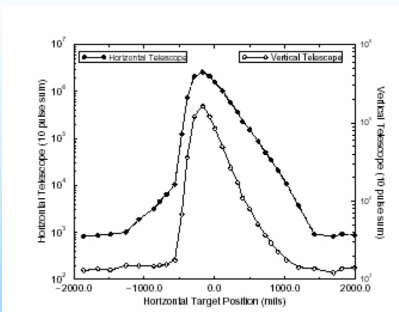

Figure 2: Horz. and Verti. Telescope triples for Horz. Scan

Solid angle remains the same through scan
Narrow acceptance, reduces noise.
Telescope acceptance about 10^{-4} steradian.

Wire Scanners

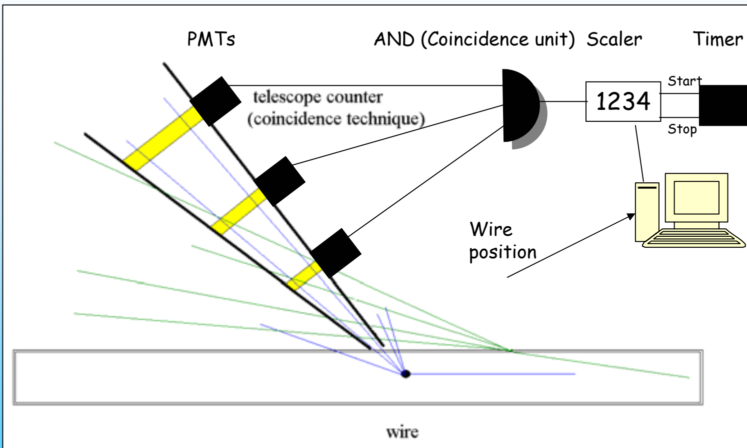

Normalize counts to time interval!
Reduced background from dark counts and beam losses

Wire Scanners at Jefferson Lab

Huge dynamic range (10^8) by coincident counting:

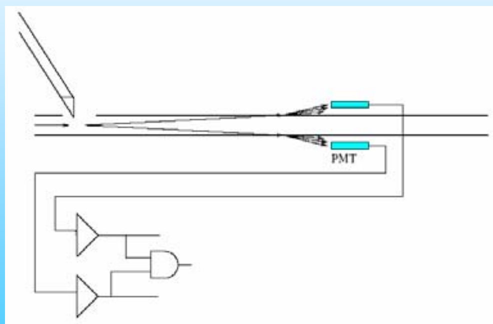

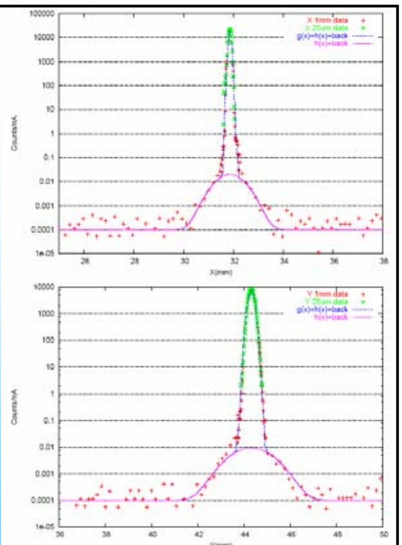

Figure 4: Beam Profile combining the 25μm and 1mm Fe wire data. The top(bottom) plot shows the X(Y) data and results of the fit to the data. The red points represent the 1mm wire data, the green points the 25μm wire data, the blue curve is the overall fit to the data and the red curve is the halo portion of the fit. The ordinate is plotted with a log-scale and the count rate is normalized to the beam current.

Wire Scanners at HERA

Huge dynamic range by scanning + counting
No scraping, single scintillator! (HERA):
Very clean beam conditions (no losses)
No halo,
even smaller than gaussian.

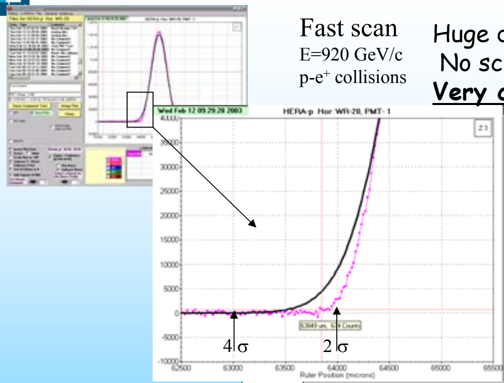

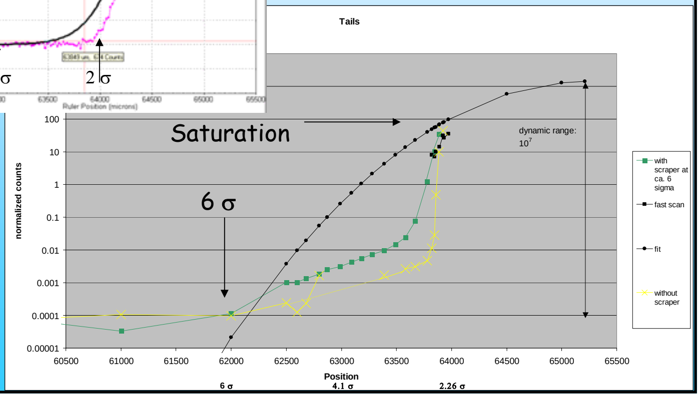

Wire Scanners at HERA

Saturation effects

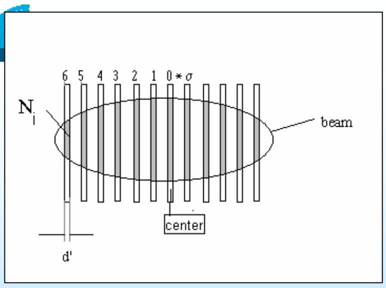

$$N_i = n_{bunch} \cdot \int_{i\cdot\sigma-\frac{d'}{2}}^{i\cdot\sigma+\frac{d'}{2}} \frac{1}{\sigma_h \cdot \sqrt{2\cdot\pi}} \cdot \exp\left(\frac{-x^2}{2\cdot\sigma_h{}^2}\right) dx$$

N = **protons intersecting wire area**
σ = beam width (0.527 mm)
d' = wire diameter (7 mm)
N_{bunch} = 2.8 * 10^{10} protons
Bunch Rate R_B = 10.4 MHz
limits the max count rate

Signal efficiency of ε=10^{-7}
Eff = N · ε, Signal Rate S = Eff · R_B

Rate: [Counts/bunch] [Counts/s]

Position	N_i =	Eff_i =	S_i =
Center	$1.484\cdot10^{8}$	14.837	$1.543\cdot10^{8}$
1 σ	$8.999\cdot10^{7}$	8.999	$9.359\cdot10^{7}$
2 σ	$2.008\cdot10^{7}$	2.008	$2.088\cdot10^{7}$
…	$1.648\cdot10^{6}$	0.165	$1.714\cdot10^{6}$
Useful range	$4.978\cdot10^{4}$	$4.978\cdot10^{-3}$	$5.177\cdot10^{4}$
	553.033	$5.53\cdot10^{-5}$	575.154
6 σ	2.26	$2.26\cdot10^{-7}$	2.351
	$3.399\cdot10^{-3}$	$3.399\cdot10^{-10}$	$3.534\cdot10^{-3}$
	$1.88\cdot10^{-6}$	$1.88\cdot10^{-13}$	$1.955\cdot10^{-6}$
	$3.825\cdot10^{-10}$	0	$3.978\cdot10^{-10}$
	$2.864\cdot10^{-14}$	0	$2.978\cdot10^{-14}$

Saturation

Lower limit

Scraping by collimators

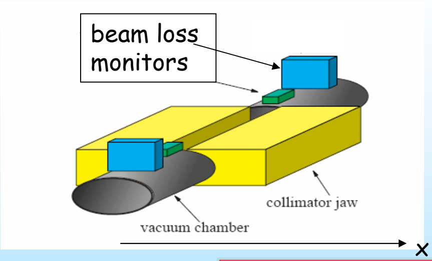

In a synchrotron one jaw will scrape both sides of the beam distribution (β-oszillation)
=> meas. symmetric halo
Such a tail scan yields information about particles which oscillate with an amplitude larger than the position of the collimator

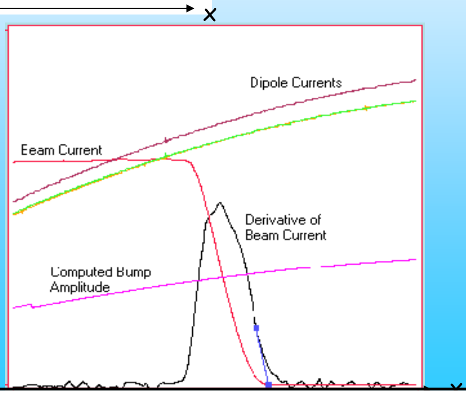

Scraping by collimators + BLM

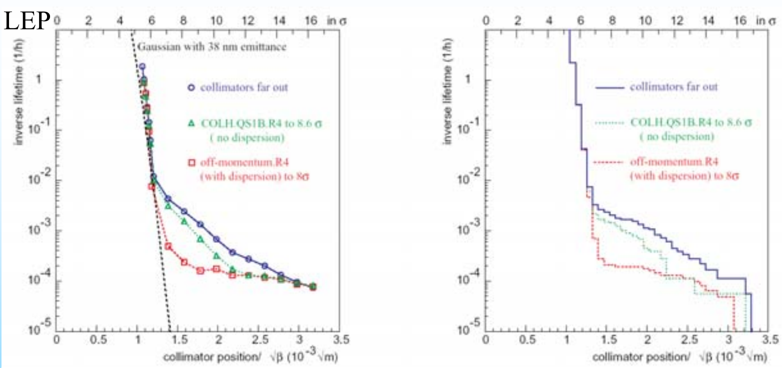

Measurement (left) and simulation (right) of the horizontal beam tails for a beam energy of 80.5 GeV and for different collimator settings at LEP. The simulation is the result of tracking particles after Compton scattering on thermal photons (black body radiation of vacuum chamber).

Measurements were performed by moving one jaw of a collimator closer to the beam in steps. Beam current and beam size measurements were recorded for each collimator setting. The collimators were moved closer until significant lifetime reductions were observed. Lifetimes calculated from beam currents for these points were used to calibrate the loss monitors. This allows to give loss rates directly in terms of equivalent lifetimes

Other sensitive, high dynamic halo monitors

Ion chamber, SEM

- Direct measurement by inserting monitor or by an intercepting monitor

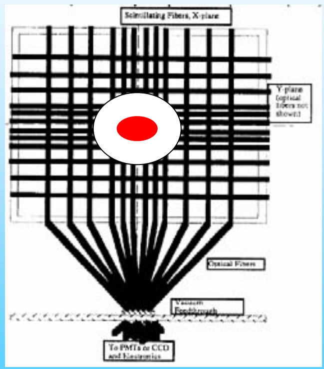

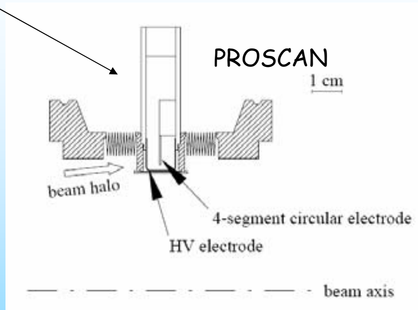

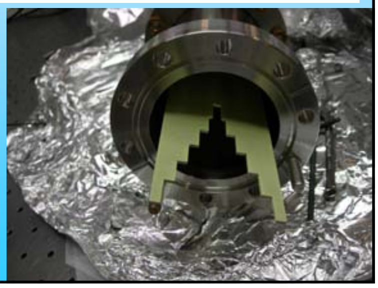

But a normalization to the beam core has still to be done (like in scraping measurement.

JLab FEL

Vibrating wire scanner

VWS mounted on the vacuum below with 1 μm step motor feed

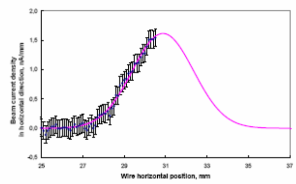

Scan of the electron beam at the Injector of Yerevan Synchrotron with an average current of about 10 nA (after collimation) and an electron energy of 50 MeV

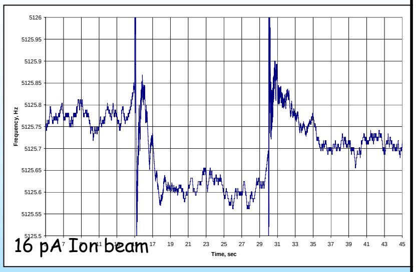

16 pA Ion beam

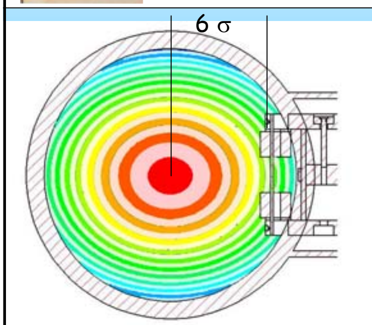

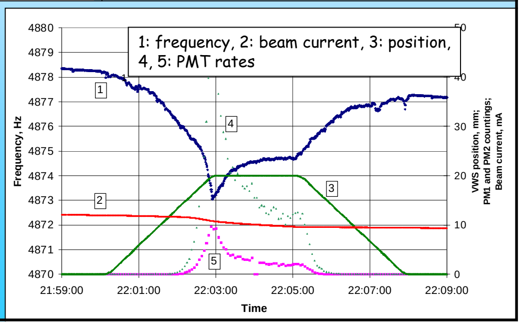

Vibrating wire scanner

Farady Cup Award: May 2008!
Yerevan Physics Institute
S.Arutunian,
VIBRATING WIRE SENSORS
FOR BEAM INSTRUMENTATION
BIW 2008, Lake Tahoe, USA

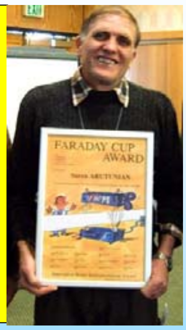

Outline

- Halo diagnostic:
  - What is Halo?
  - Halo Quantification
- Transversal Halo Measurements with:
  - Wire Scanners and Scrapers (slow)
  - **Optical Methods (fast)**
- Longitudinal Halo
  - Bunch Purity,
  - "Beam in Gap"
  - Coasting Beam

Optical methods

Light generation by SR, OTR, Phosphor screens, …

Very fast compared with scanning methods

- Large dynamic range readout
  - CID camera
  - Micro Mirror Array
- Halo measurements with coronagraph

CID Camera

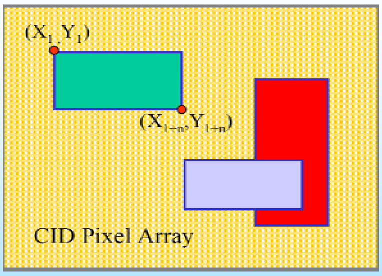

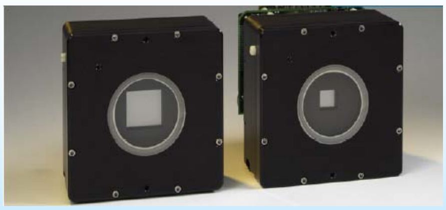

Commercial available

http://www.thermo.com/eThermo/CMA/PDFs/Product/productPDF_26754.pdf

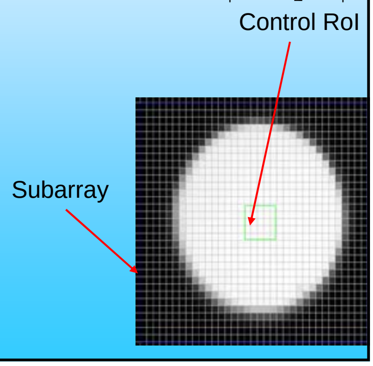

Each pixel on the CID array is individually addressable and allows for random access non-destructive pixel readout. The *random access integration* (RAI) mode **automatically adjusts the integration time from pixel to pixel based upon the real-time observation of photon flux** using CID random accessibility and non-destructive readout. With this RAI mode a dynamic range (~10^6) can be achieved.

Comparison

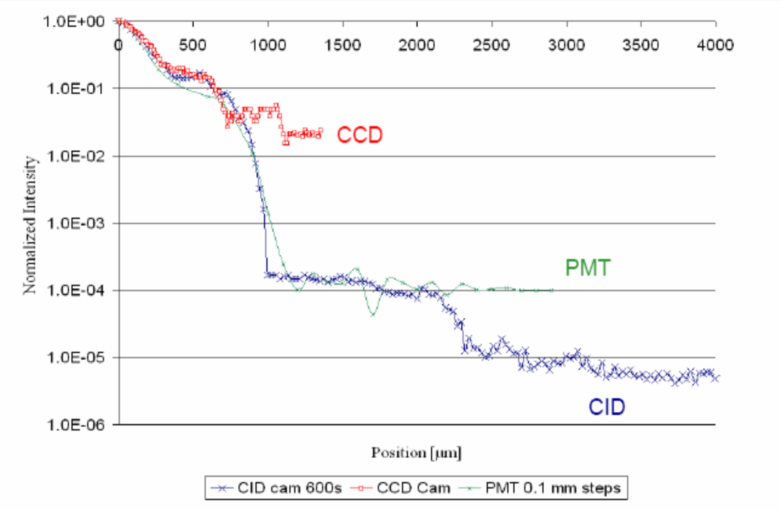

Optical methods

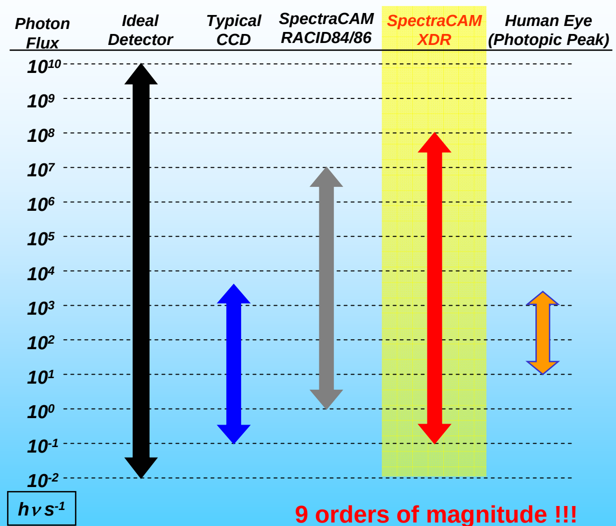

SPECTRACAM XDR: High resolution scientific imaging camera system using Charge Injection Device capable of extremely high dynamic range and random pixel addressing

Micro Mirror Array

- 1024 x 768 pixels (XGA)
- USB Interface
- high-speed port 64-bit @ 120 MHz for data transfer
- up to 9.600 full array mirror patterns / sec (7.6 Gbs)
- 16 µm in size
- +/- 10° of rotation
- Switch of 15 µs physically, 2 µs optically

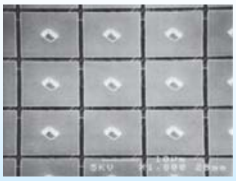

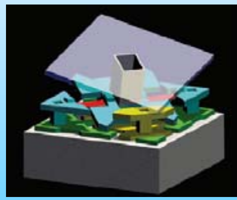

The first applications were in digital projection equipment, which has now expanded into digital cinema projectors, with sometimes **more than two million micro mirrors per chip switching at frequencies of up to 5 kHz**. Recently MMAs are finding applications in the large telecommunications market as optical multiplexers and cross-connect switches.

Micro Mirror Array

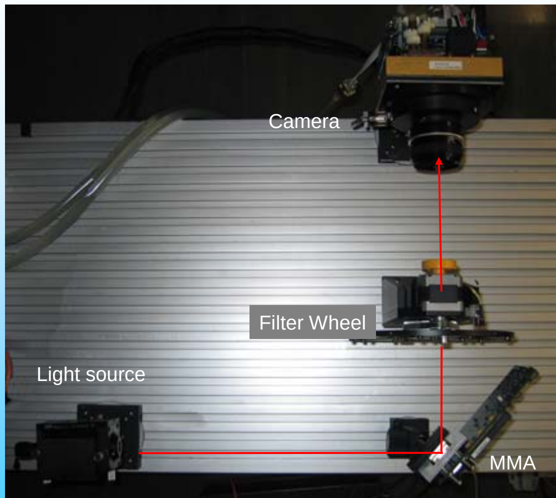

Micro Mirror Array

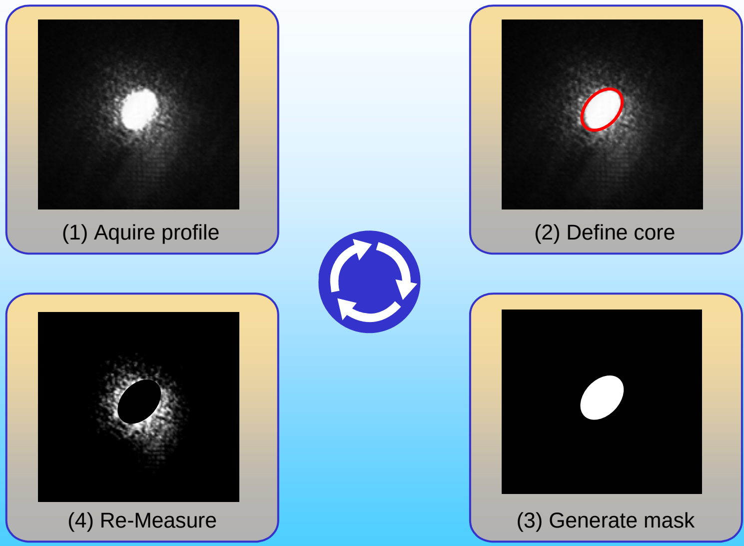

Optical methods

Directional optical radiation (e.g. Synchrotron radiation or OTR) with small opening angles ($\approx 1/\gamma$) suffer from diffraction limits:

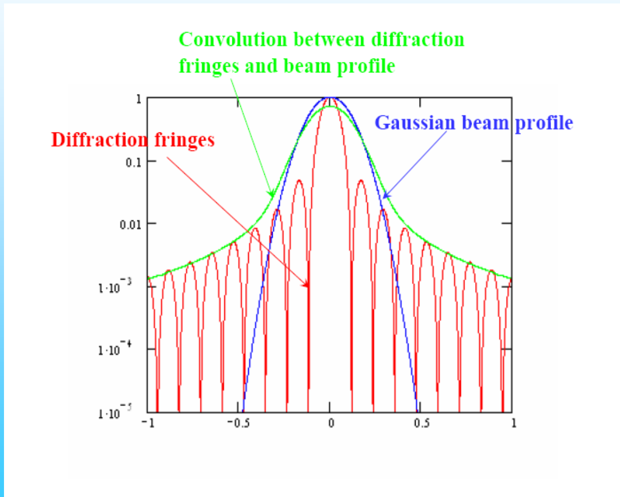

Halo measurements with coronagraph

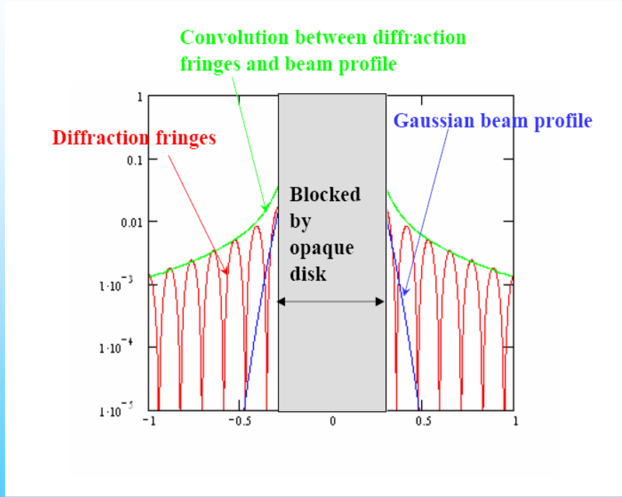

Halo measurements with coronagraph

A **coronagraph** is a telescopic attachment designed specifically to block out the direct light from a star, so that nearby objects can be resolved without burning out the telescope's optics. **Most coronagraphs are intended to view the corona of the Sun**, The coronagraph was introduced in 1930 by the astronomer Bernard Lyot.

The simplest possible coronagraph is a simple lens or pinhole camera behind an appropriately aligned occulting disk that blocks direct sunlight; **during a solar eclipse, the Moon acts as an occulting disk and any camera in the eclipse path may be operated as a coronagraph until the eclipse is over.**

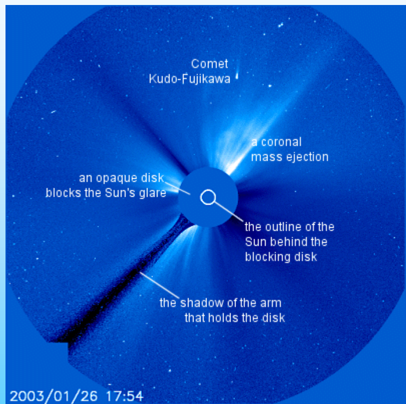

http://en.wikipedia.org/wiki/Coronagraph

Halo measurements with coronagraph

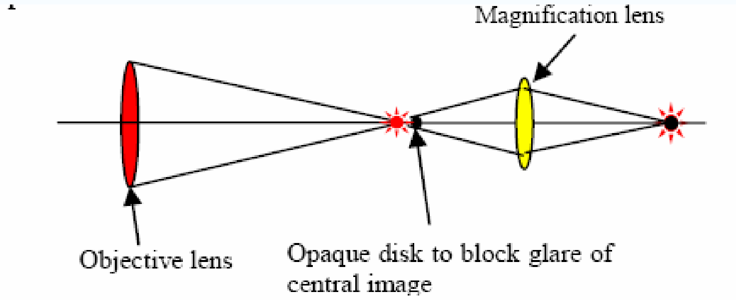

Set up of normal telescope with opaque disk.

When using OTR or SR (narrow cone) the diffraction fringes makes tail surrounding from the central beam image. Intensity of diffraction tail is in the range of 10^{-2} -10^{-3} of the peak intensity. The diffraction tail disturb an observation of week object surrounding from bright central beam

Following pictures from a talk:
BEAM HALO OBSERVATION BY CORONAGRAPH. T. Mitsuhashi, DIPAC 2005
Photon Factory storage ring

Halo measurements with coronagraph

Lyot's brilliant idea for the coronagraph is to remove this diffraction fringe by a mask, and relay the hidden weak image by a third lens onto the final observation plane

The Lyot stop effectively remove the diffracted light halo that surrounds the target, giving higher contrast improvement.

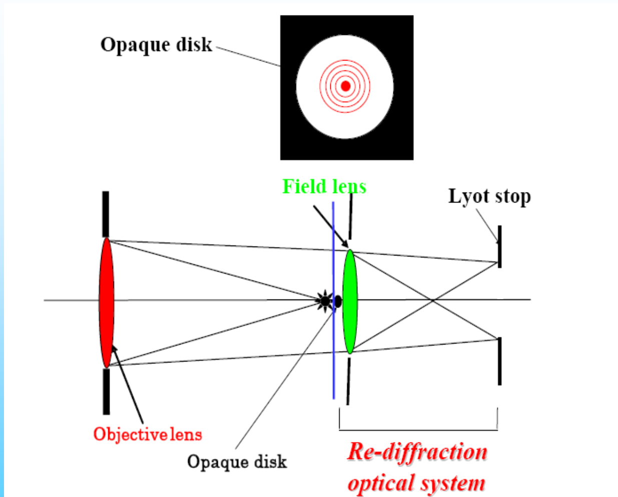

The first lens (objective lens) makes a real image of the object (beam image) on to a blocking opaque disk

Halo measurements with coronagraph

Lyot's brilliant idea for the coronagraph is to remove this diffraction fringe by a mask, and relay the hidden weak image by a third lens onto the final observation plane

The Lyot stop effectively remove the diffracted light halo that surrounds the target, giving higher contrast improvement.

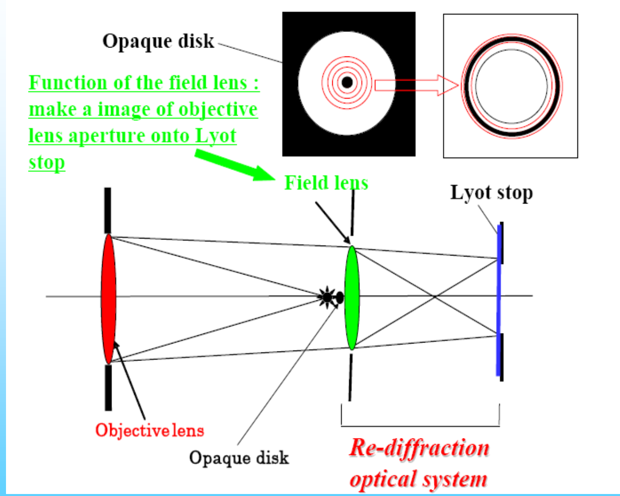

A second lens (field lens) is set just after the blocking disk. The focusing length of the field lens is chosen to make a real image of the objective lens aperture onto a mask (Lyot Stop).

Halo measurements with coronagraph

Lyot's brilliant idea for the coronagraph is to remove this diffraction fringe by a mask, and relay the hidden weak image by a third lens onto the final observation plane

The Lyot stop effectively remove the diffracted light halo that surrounds the target, giving higher contrast improvement.

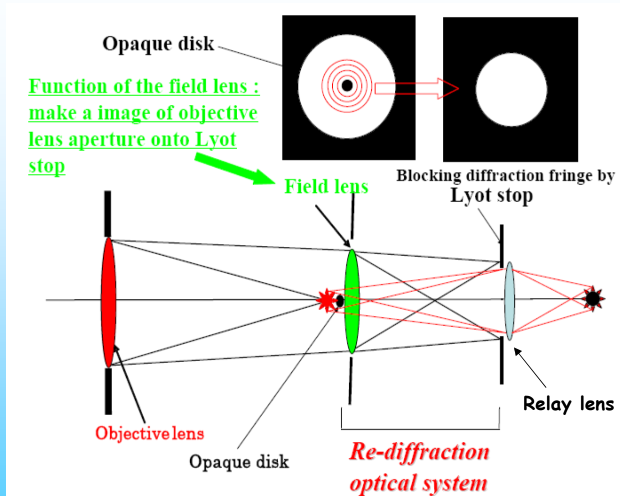

Then the re-diffracted light makes another diffraction fringe around the geometrical image of the objective lens aperture in the focal plane of the field lens. The Lyot stop removes this diffraction fringe by a mask, and relay the image by a third lens onto the final observation plane.

Halo measurements with coronagraph

expected dynamic range: 10^6 - 10^7

Zoom up of opaque disk.

Shape is cone and top-angle is 45°

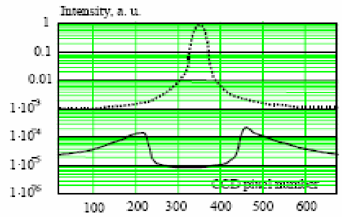

Figure 2: Coronagraph test. Upper curve is a source image. The down curve is the source obscured by mask.

VEPP3

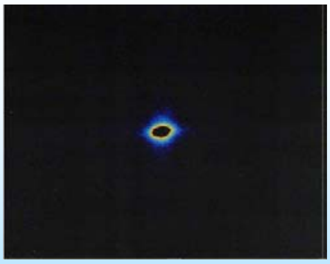

Beam profile

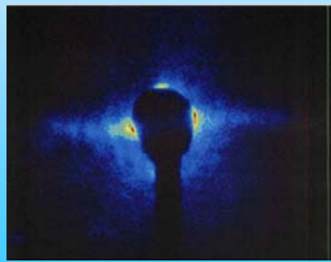

Beam tail

Halo measurements with coronagraph

Observation for the more out side

Single bunch 65.8mA

Exposure time of CCD : 3msec

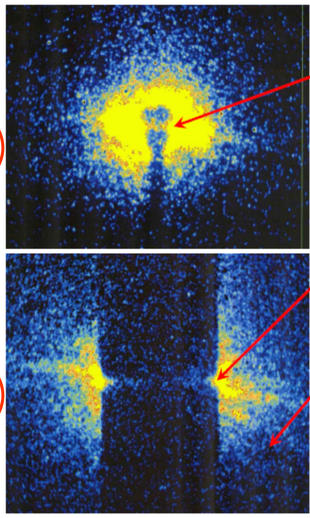

Intensity in here : 2.05×10^{-4} of peak intensity

2.55×10^{-6}

Far tail

Exposure time of CCD : 100msec

Background leavel : about 6×10^{-7}

Halo measurements with coronagraph

Background sources
1.Scattering by defects on the lens surface (inside) such as scratches and digs.
2. Scattering from the optical components (mirrors) near by coronagraph.
3. Reflections in inside wall of the coronagraph. Cover the inside wall with a flock paper (light trapping material).
4. Scattering from dust in air. Use the coronagraph in clean room.

A background level of $6 \cdot 10^{-7}$ and a spatial resolution of 50 μm was achieved.

LIMITATIONS
• OTR light intensity was not intense enough to explore further the halo distribution (CTF3).
• The masking technique must follow the beam position and halo size to avoid the saturation of the camera.

Dust and impurities on lenses

Outline

- Halo diagnostic:
  - What is Halo?
  - Halo Quantification
- Transversal Halo Measurements with:
  - Wire Scanners and Scrapers (slow)
  - Optical Methods (fast)
- Longitudinal Halo
  - **Bunch Purity:** Time-Correlated Single Photon Counting (TCSPC)
  - "Beam in Gap"
  - Coasting Beam

Bunch Purity Measurements

Measurement of the sometimes special fill pattern of synchrotron light sources (rings) is important for the time-resolved experiments. **The adjacent buckets must not have any stored particles or, in reality, as few as possible.** A method with very good time resolution (<< 1ns for a 500 MHz RF-System) and high dynamic range (more than six orders of magnitude) is necessary.

Mechanism of loosing electrons

1) Quantum lifetime. An electron is lost from a bucket by emitting a photon having a momentum larger than bucket heigth η_{RF} and can be captured by the backward buckets.

2) Lifetime determined by the vacuum pressure. Electrons lose energy by collisions with residual gas molecules in the vacuum chamber.

3) Touschek effect. Electrons in a bunch execute betatron oscillation with transverse momenta. When two electrons are scattered elastically (Moller scattering), the transverse momenta can be transferred to longitudinal ones.

4) Injection errors (energy, timing,). At top-up a source of impurity growth on the both time sides of the main rf buckets.

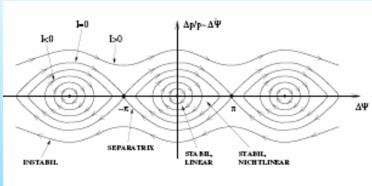

A typical measurement is a time-correlated single photon counting method (TCSPC):

TCSPC

Time-correlated single photon counting method

PETRA II setup:
"The parasitic bunch measurement is achieved by an avalanche-photo diode (APD) detecting scattered X-rays from a 1 mm thick graphite foil. It is located in the PETRA beamline 31.3 m downstream of a dipole used as x-ray source. The detector signals are amplified close to the diode by a fast amplifier. "
The detector must be carefully shielded against stray light.

ESRF Setup

http://www.esrf.eu/Accelerators/Groups/Diagnostics/BunchPurityMeasurements

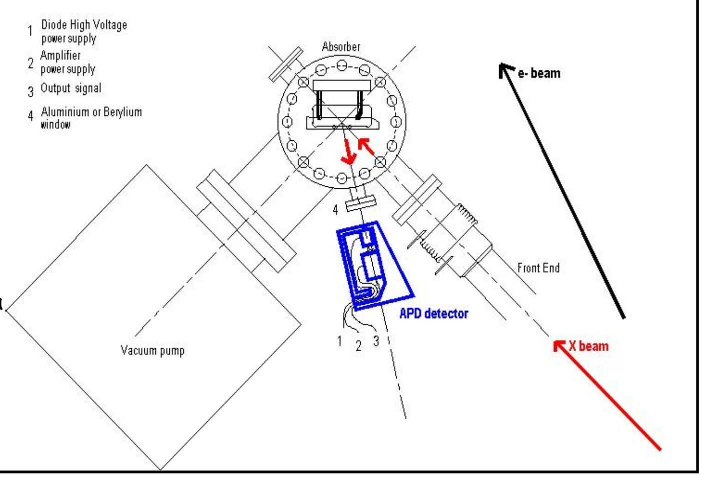

TCSPC

The **arrival time of single photons** emitted by the electron bunches passing through a particular dipole in the storage ring **is measured**. The photon arrival time is measured relative to a clock pulse which is **synchronized to the bunch revolution** frequency via the storage ring RF system.

The amplified signal is analyzed using a time-to-digital-converter (**TDC**) and a multichannel-analyzer (**MCA**). To reduce the influence of the so-called "walk" and to reduce the background due to electronic noise the amplified detector signal is filtered by a constant-fraction-discriminator (CFD).

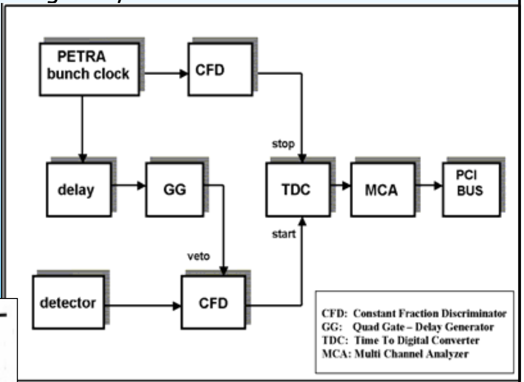

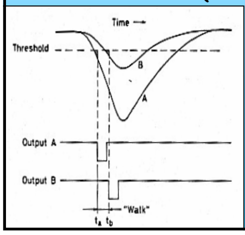

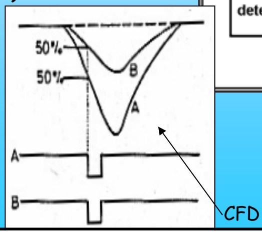

TCSPC

The TDC-board offers 4096 channels with minimum width below **40 ps** and can work at **count rates up to 3 MHz** (300 ns recovery time).
To measure a histogram not affected by recovery-time and pile-up effects, the detector count rate should be limited to below 1.5% of the sync rate.

Bunch distance = 10 MHz, count rate = 10 kHz, expected dynamic range: 10^7
=> time to resolve $1/10^7$ = 100 sec, with better statistic => 1000 s ≈ **16 min!!!!**

TCSPC

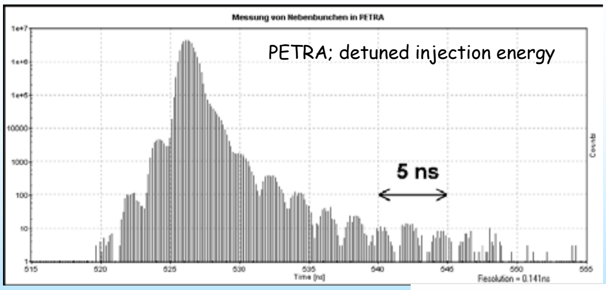

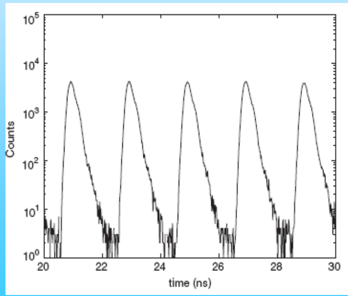

Each bucket filled (500 MHz)

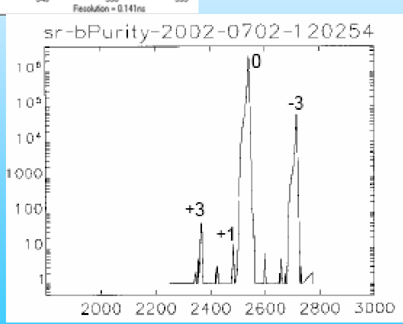

APS, 352 MHz RF, after 98 hours top-up operation

TCSPC

Improvements:

1) Better TDC: The HydraHarp 400 ps event timer & TCSPC .The system features a time resolution down to **1 ps**,... A common sync input for all channels permits to use the system for TCSPC in forward start-stop mode at stable excitation sources up to **150 MHz**.

2) Use of **MCP-PMT** for better detector timing

http://www.picoquant.com/_instrumentation.htm

APD (C30703F) (534X LC)  vs. 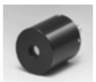 MCP-PMT (R3809U-50)

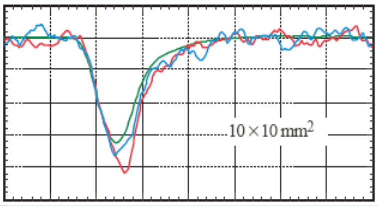

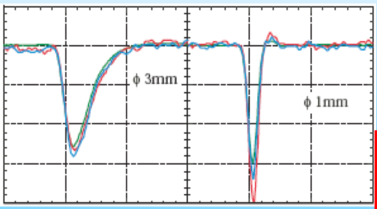

APD: The average over many events is shown (smooth curve) as well as two single-photon events to show an indication of the noise level
Scale: 50 mV (upper) 100 mV (lower) and
5 ns /div.

typ. dark count rate 20-500 c/s

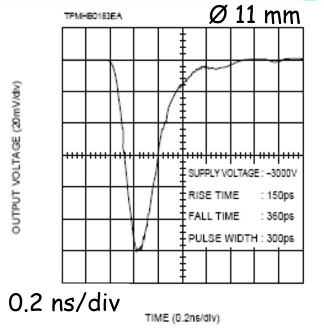

0.2 ns/div

Dark count rate limits the dynamic range in a 100 ns interval to ≈10^7

100 c/s

Figure 5: Variation of Dark Counts Depending on Ambient Temperature

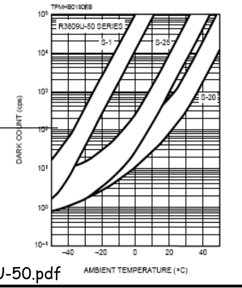

http://datasheet.digchip.com/190/190-01565-0-R3809U-50.pdf

TCSPC

Instrumental effects:

Pile up:

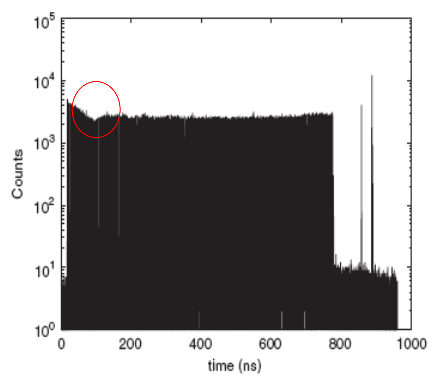

The number of electrons is nearly the same in the bunches of the train, but the measurement shows a decreasing number in the first bunches, down to a minimum value, followed by a flat top for the rest of the bunches. This effect is due to a **too high count rate** of 4.5 ·10^6 counts/s. At this rate, a photon arrives every 220 ns on average: this is **comparable to the dead time** of the PicoHarp 300 (95 ns). As a result the probability of a photon from one of the first pulses to be detected is significantly larger than for the rest of the train.

TCSPC

Instrumental effects:

Instrument response function:

MCP-PMT after pulses

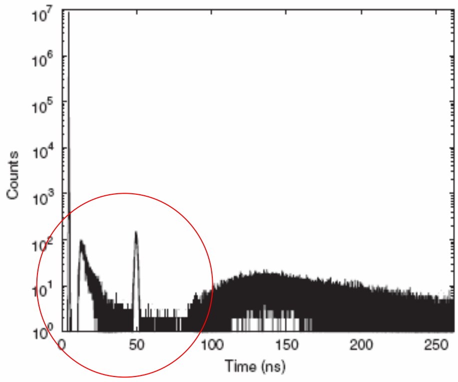

Fig. 4. Full scale of the IRF recorded with the 35 ps diode, with approximatively 1 count/s noise.

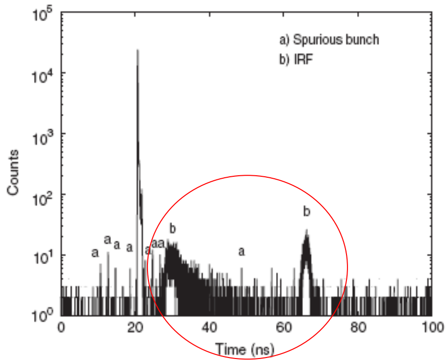

Fig. 5. SRS single bunch mode pattern at 600 MeV. Due to a small current (4 mA) the count rate is only 3000 and the background is 100 counts/s. Spurious bunches (a) can be seen in the adjacent buckets of the main bunch, and the after-pulses of the MCP-PMT (b) as observed in the IRF.

TCSPC

Spring-8:
Huge dynamic range with fast optical light shutters (Pockels cells), selecting only one bucket.
Measuring time: 500 s for satellites.
Main peak is suppressed by 10^{-5} due to shutter efficiency.

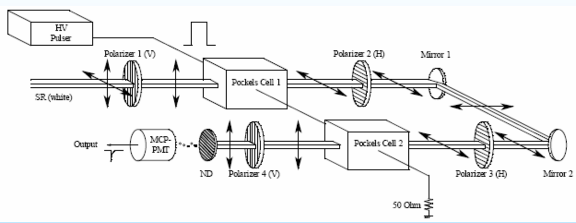

=> **Dynamic range ≈10^{10}!**

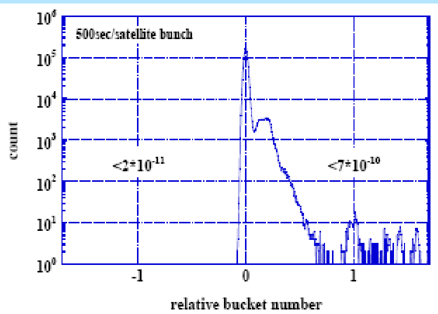

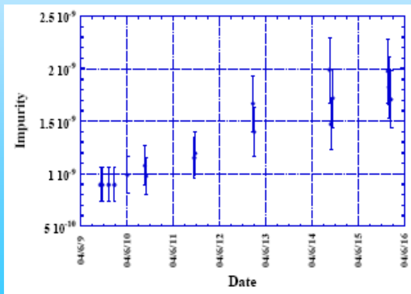

Growth of bunch impurity during top up at Spring-8

Outline

- Halo diagnostic:
  - What is Halo?
  - Halo Quantification
- Transversal Halo Measurements with:
  - Wire Scanners and Scrapers (slow)
  - Optical Methods (fast)
- Longitudinal Halo
  - Bunch Purity
  - **"Beam in Gap"**
  - **Coasting Beam**

} by Temporal Loss Distribution / Synchrotron Radiation

Beam in Gap

Proton storage rings

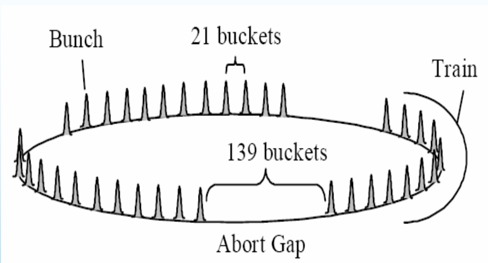

If beam (AC or DC) in gap, extraction kicker ramp will spray beam ➔ will result in:
- Quenches (SC-magnets)
- activation
- spikes in experiments
- equipment damage
- …

Beam in Gap (hadrons) due to:
- Injection errors (timing)
- debunching
- diffusion
- RF noise/glitches
- …

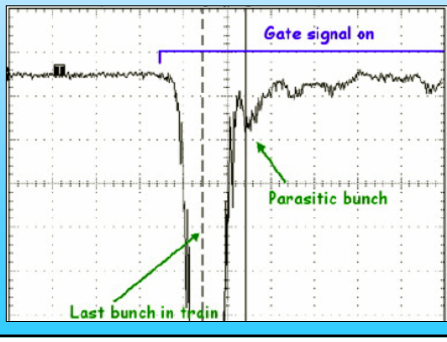

Beam in Gap

Proton Synchrotron Light (Tevatron, LHC)

Successful test at ALS for LHC with gated MCP/PMT (AC beam),

More tests at TEVATRON with MCP-PMT in counting mode (more sensitive, DC beam),

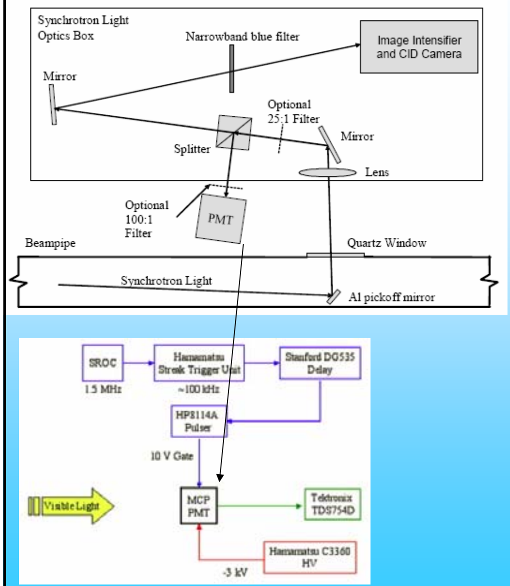

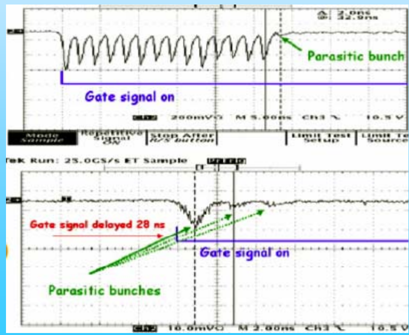

Beam in Gap

Proton Synchrotron Light (Tevatron, LHC)

Successful test at ALS for LHC with gated MCP/PMT (AC beam),

More tests at TEVATRON with MCP-PMT in counting mode (more sensitive, DC beam),

Studies with Single-Photon Avalanche Detectors for LHC are ongoing

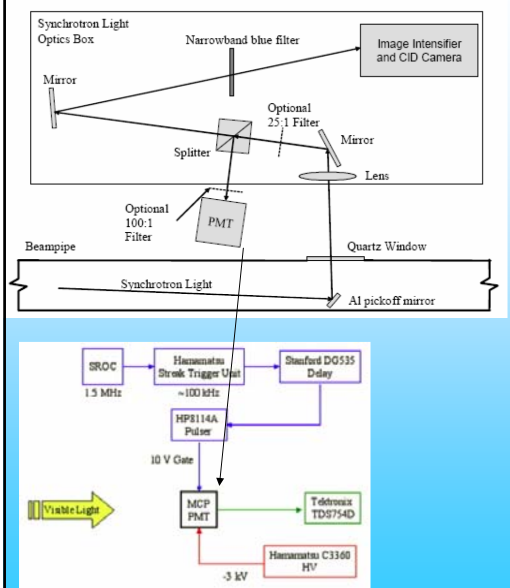

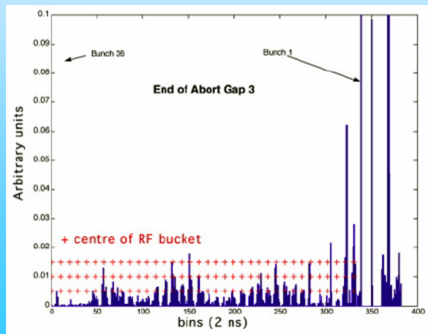

Coasting beam

Hadron beams, rings

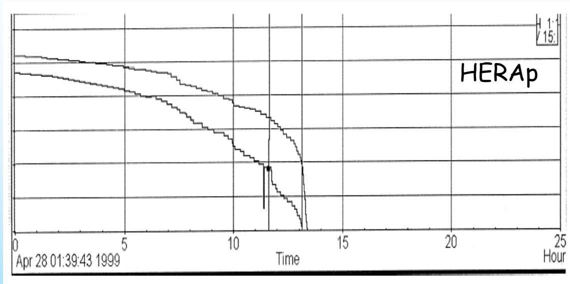

DC current (upper) and total bunch current (lower)

Tevatron: 980 GeV protons and antiprotons lose about 9 eV/turn due to the SR. For **uncaptured beam particles**, this energy loss is not being replenished by the rf system, so they **slowly spiral radially inward and die on the collimators**, which determine the tightest aperture in the Tevatron during collisions. The typical time for an uncaptured particle to reach the collimator is **about 20 minutes. The total uncaptured beam intensity is a product of the rate at which particles leak out of the main bunches and the time required for them to leave the machine.**

PHYSICAL REVIEW SPECIAL TOPICS - ACCELERATORS AND BEAMS **11**, 051002 (2008), **Generation and diagnostics of uncaptured beam in the Fermilab Tevatron and its control by electron lenses, by** Xiao-Long Zhang et al

Coasting beam

Measured by temporal beam loss distribution

HERA-B: Wire scanners + Counters + TDC (only in beam tails)

Uncertainty due to meas. in halo!

Detection efficiency > 50%

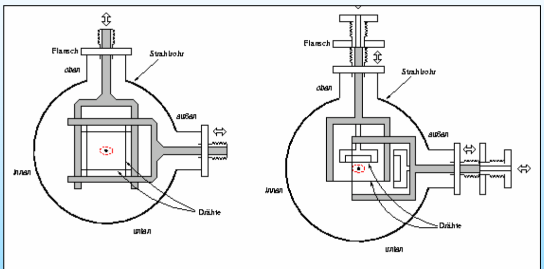

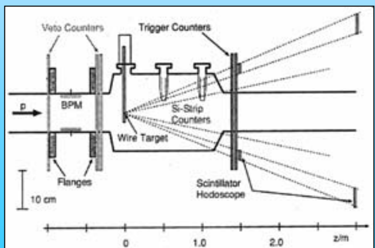

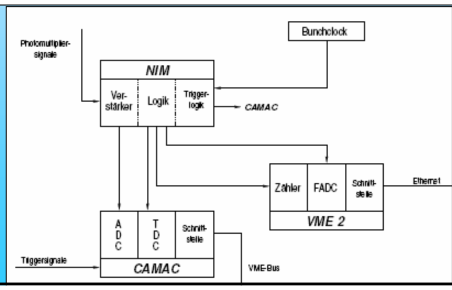

Coasting beam

Detection of coasting beam

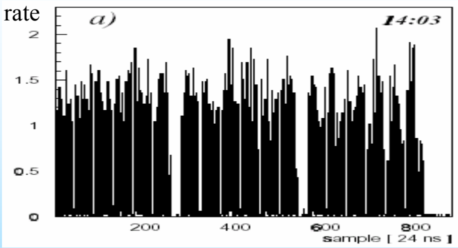

1 h

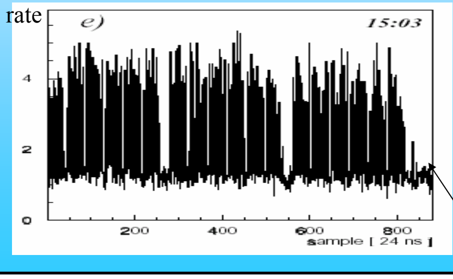

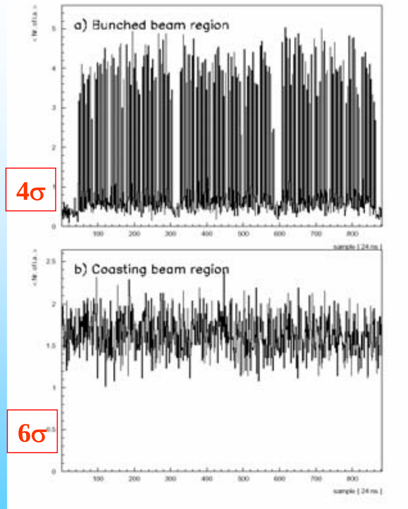

Figure 11.2: The time structure of the proton interaction for an outer target wire at different distances of the wire to the beam center: a) wire $\approx 4\sigma$ from the beam center and b) wire $\geq 6\sigma$ from the beam center.

Note the increased rate in the Bunch gaps (=coasting beam)

Coasting beam and bunch impurity

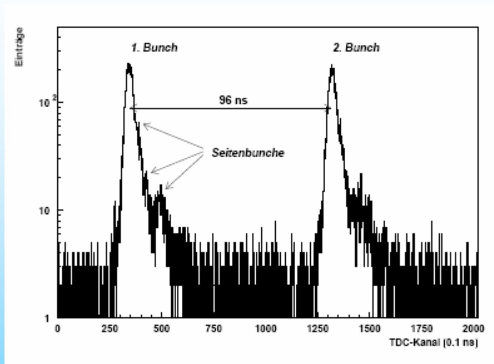

Another method: Fast wall current monitor

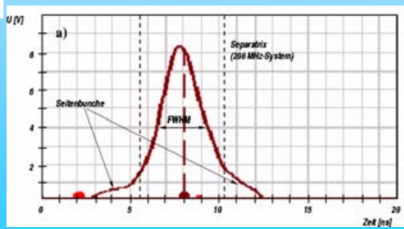

Coasting beam

CDF (FNAL): "normal" losses + Counter + variable Trigger delay

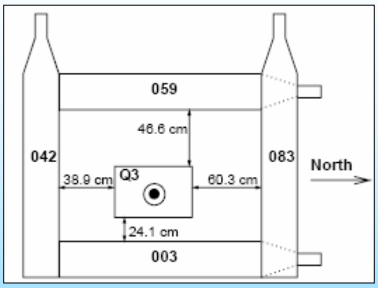

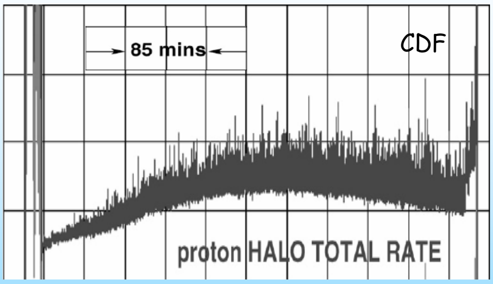

Outline

- Halo diagnostic:
  - What is Halo?
  - Halo Quantification
- Transversal Halo Measurements with:
  - Wire Scanners and Scrapers (slow)
  - Optical Methods (fast)
- Longitudinal Halo
  - Bunch Purity,
  - "Beam in Gap"
  - Coasting Beam

} not mentioned: Abort Gap Cleaning by
Kickers (fast or resonant)
Electron lens

Summary

Transversal Halo

- Wire scanners still "state of the art" instruments for very high dynamic range up to 10^8 or more.
- SR with CID and coronagraph has potential to more dynamic range.
- IPM and LPM sufficient for profiles but background and instrumental issues limit use for halo.
- Laser work well for H^- beams.

Longitudinal Halo

- Bunch purity measurements with >10^{10} dynamic range
- Beam in Gap: SR limited to high energy beam
- Wire scanners are very sensitive but applicable in trans. halo only

References

Introduction

What is Halo

HALO ESTIMATES AND SIMULATIONS FOR LINEAR COLLIDERS, H. Burkhardt et al, EUROTeV-Report-2007-064, CLIC-Note-714
Beam halo definitions based upon moments of the particle distribution C. K. Allen, T. P. Wangler, Phys. Rev. ST Accel. Beams **5**, (2002)
Halo Diagnostics Sumary, P. Cameron, K. Wittenburg, Halo03.
RMS Emittance Measurements Using Optical Transition Radiation Interferometry at the Jefferson Lab FEL, Michael Andrew Holloway - PAC 07.
Design and Construction of a Beam Shape and Halo Monitor for the CERN SPL, K. Hanke, M. Hori, CARE/HIPPI Document-2005-005
Halo Diagnostics Overview, Tom Shea and Peter Cameron, Halo 03
Mechanisms of halo formation, A. V. Fedotov, Halo03
Overview of recent halo diagnosis and non-destructive beam profile monitoring, K. Wittenburg; HB2006

Halo Qualification

BEAM HALO IN PROTON LINAC BEAMS, T. P. Wangler et al, Linac 2000
Parameters for quantifying beam halo, C.K. Allen and T.P. Wangler, PAC 2001.
The Development of Computational Tools for Halo Analysis and Study of Halo Growth in the Spallation Neutron Source Linear Accelerator, D. A. Bartkoski et al, EPAC'06
AN EXPERIMENTALLY ROBUST TECHNIQUE FOR HALO MEASUREMENT, J. Amundson et al, FERMILAB-PUB-06-060-CD

Halo Measurements with

IPM:

A Prototype of Residual Gas Ionization Profile Monitor for J-PARC RCS, Kenichirou Satou et al, EPAC'06
DEVELOPMENT OF A PERMANENT MAGNET RESIDUAL GAS PROFILE MONITOR WITH FAST READOUT, S. Barabin et al, RuPAC04
Optical design for BIPM imaging system, B. Dehning, et al, CERN-AB-2005-072
Simulation of an electron source based calibrating system for an ionisation profile monitor, B. Dehning et al, CERN-AB-2005-073
Comparative Transverse Distribution Measurements between the New SPS Rest Gas Ionisation monitor and the wire scanner monitors, C. Fischer et al, EPAC04
The IPM as a Halo Measurement and Prevention Diagnostic, R. Connolly et al, HALO03
Scraping for LHC and collimation tests in the CERN SPS. M. Facchini et al, CERN-AB-2005-070
DESIGN STUDY OF A NONDESTRUCTIVE BEAM PROFILE AND HALOS MONITOR BASED ON RESIDUAL GAS IONIZATION FOR THE J-PARC RCS, S.Lee et al. The 14th Symposium on Accelerator Science and Technology, 2003
R&D OF BEAM MONITORS AT J-PARC NEUTRINO BEAMLINE. Ishida et al, , PAC 05
Results with the SPS Rest Gas Profile Monitor by Collecting the Liberated Electrons, C. Fischer, J. Koopman LHC Emittance Workshop – July 3-4, 2000

LPM

Development of beam position and profile monitor based on light radiation of atoms excited by the beam particles. N.I. Balalykin, et al. RuPac04
Beam Profile Measurement with CCD Camera at PEFP, S. H. Han, Y. S. Cho, APAC2004
Optical Transverse Beam Profile Measurements for High Power Proton Beams, P. Ausset, et al, EPAC02

References

Halo Measurements with

Laser

Direct Measurements of Space-Charge-Potential in High Intensity H- Beam with Laser Based Photo Neutralization Method, Seishu Lee et al, DIPAC05
SNS Laser Profile Monitor Progress, W. Bokland et al EPAC04

Scanners and Scrapers

THE HIGH-HEAT FLUX TESTING OF AN INTERCEPTIVE DEVICE FOR AN INTENSE PROTON BEAM, R. Valdiviez et al, PAC2001
ANALYSIS OF DATA FROM THE LEDA WIRE SCANNER/HALO SCRAPER, J. H. Kamperschroer et al, PAC2001
BEAM PROFILE WIRE-SCANNER/HALO-SCRAPER SENSOR ANALOG INTERFACE ELECTRONICS, M. E. Gruchalla, PAC01
Halo Measurements of the Extracted Beam at the Los Alamos Proton Storage Ring, A. Browman et al, PAC 1993
Large Dynamic Range Beam Profile Measurements, A.P. Freyberger, DIPAC05
Scintillator Telescope in the AGS Extracted Beamline , D. Gassner et al., HALO03
Beam Tail Measurements using Wire Scanners at DESY, K. Wittenburg et al, HALO03
Transverse Beam tails Due To Inelastic Scattering, H. Burkhardt, I. Reichel, G. Roy, CERN-SL-99-068
BEAMSCOPE - A NOVEL DEVICE FOR MEASURING EMITTANCES AND BETATRON AMPLITUDE DISTRIBUTIONS H. Schonauer , IEEE-NS.26, 1979
THE ELECTRON DISTRIBUTION IN HERA AND THE CONSEQUENCES FOR THE H1 DETECTOR AFTER THE LUMINOSITY UPGRADE, A. Meseck, DESY-THESIS-2000-042
Beam Diffusion Studies at RHIC, R.P. Fliller III, et al, EPAC02
Profile, Current, and Halo Monitors of the PROSCAN Beam Lines, Rudolf Dölling, BIW 2004
A Scintillating Fiber Beam Halo Detector for Heavy Ion Beam Diagnostics, McMahan, M.A. et al, PAC 1993
PETRA PROTON BEAM PROFILING BY VIBRATING WIRESCANNER. S.G.Arutunian et al, DIPAC 2005

Optical methods:

BEAM HALO OBSERVATION BY CORONAGRAPH. T. Mitsuhashi DIPAC 2005
STUDY OF BEAM TAILS WITH THE OPTICAL CORONAGRAPH, O. I. Meshkov et al, EPAC04
BEAM HALO MONITORING AT CTF3; T. Lefèvre et al, EPAC04
C.P. Welsch, talks given at CLIC meeting, 16.3.2007 and CLIC BDS day – CERN , 2005
High Dynamic Range Beam Profile Measurements; C. P. Welsch et al., EPAC'06
OPERATIONAL EXPERIENCE WITH A CID CAMERA SYSTEM, C.P. Welsch et al., CLIC Note 657, 2006
Design Alternatives for Beam Halo Monitors in High Intensity Accelerators, C.P. Welsch et al, DIPAC 2005
Alternative techniques for beam halo measurements.C.P. Welsch et al, Measur.Sci.Tech.17,2006
CTF3 Instrumentation, T. Lefevre, talk at BIW08, Lake Tahoe

References

Longitudinal Halo

Bunch purity

Two Notable APDs for Fast X-ray Detection, A.Q.R. BARON, et al, SPring-8/JASRI, http://www.spring8.or.jp/pdf/en/ann_rep/99/p149-150.pdf
Bunch Purity Measurement for Diamond, C.A. Thomas et al., NIM A,566(2) 762766, October 2006.
BUNCH CLEANING STRATEGIES AND EXPERIMENTS AT THE ADVANCED PHOTON SOURCE, N. S. Sereno,y, PAC 1999
SINGLE BUNCH PURITY DURING SPRING-8 STORAGE RING TOP-UP OPERATION, K. Tamura, et al, 1st Annual Meeting of Particle Accelerator Society of Japan and the 29th Linear Accelerator Meeting in Japan
Bunch Purity Evolution during APS Storage Ring Top-up Operations, A.H. Lumpkin., et al, PAC2003
PARASITIC BUNCH MEASUREMENT IN e+/e– STORAGE RINGS, H. Franz et al, DIPAC 2003
Measurement of the longitudinal bunch structure in the Photon Factory positron storage ring with a photon counting method, Obina T et at, NIM 354, Nr. 2, 1995

Beam in GAP

Gated Microchannel Plate Photomultipliers For Longitudinal Beam Diagnostics, Stefano De Santis et al, BIW 2006.
Measurement of the intensity of the beam in the abort gap at the Tevatron utilizing synchrotron light., R. Thurman-Keup, et al, FERMILAB-CONF-05-139 2005
Development of an abort gap monitor for the Large Hadron Collider. J.F. Beche,et al, LBL-55208, 2004
Design of an Abort Gap Monitor for the Large Hadron Collider, J.-F. Beche et al, LARP Note 1, CBP Tech Note – 329, 2005
Single photon detector tests for the LHC synchrotron light diagnostics. S. Hutchins et al, DIPAC 2005
Bestimmung der Wechselwirkungsrate des HERA-B Targets und Untersuchung des Coasting Beam am HERA Protonen-Ring, Stefan Spratte, Thesis, 2000

And ...

Halo Measurements with Ionization Profile Monitors

(IPM)

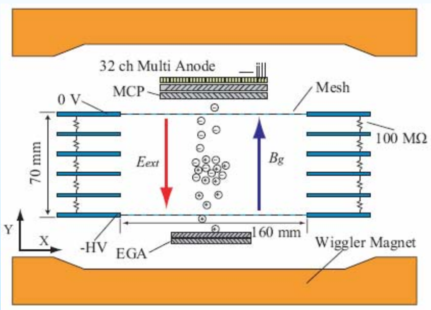

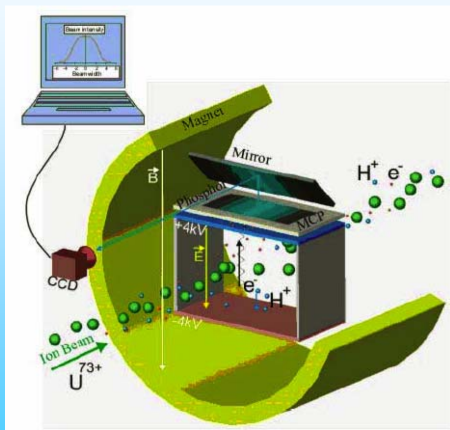

Modern IPMs use strong magnet field B_g and high voltage ($E_{ext} \leq$ 100 kV/m) to overcome space charge distortion!

However typical strength of the electric field is about 250kV/m around the beam.

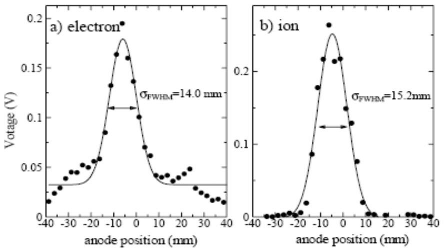

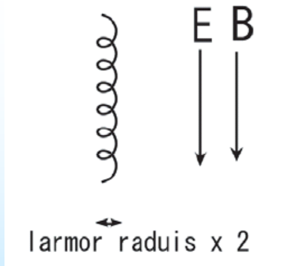

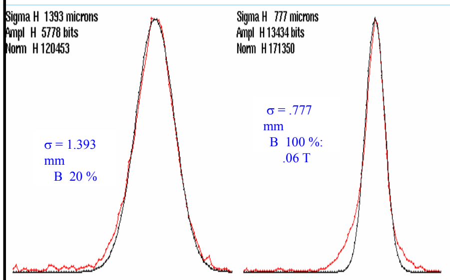

electron collection

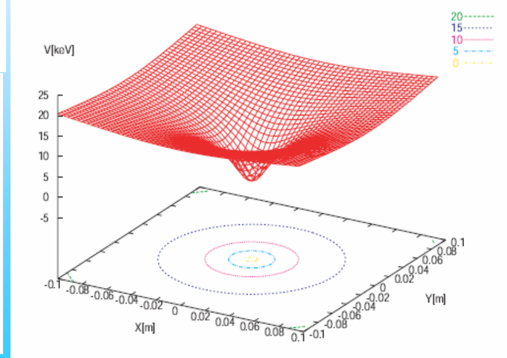

Calculated electrical potential of the J-PARC proton beam.

Ionization Profile Monitor

Emphasis on

1. Development of a proper electromagnetic guiding system design (transversal **and** longitudinal) for sub-mm resolution.
2. New MCP calibration scheme with EPG (Electron Generator Plate (Burle Inc.) or tungsten filaments

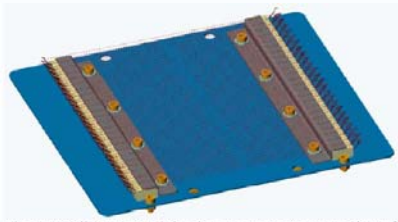

Figure 6: Filament module, the center to center spacing of two wires is 3mm.

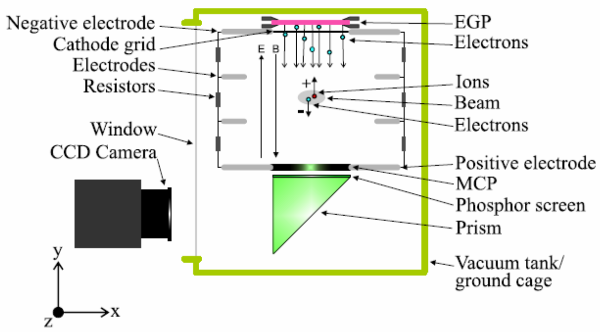

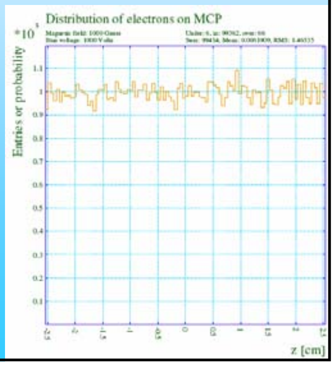

Ionization Profile Monitor

3) Improved optical design done with the ZEMAX Program (CERN)

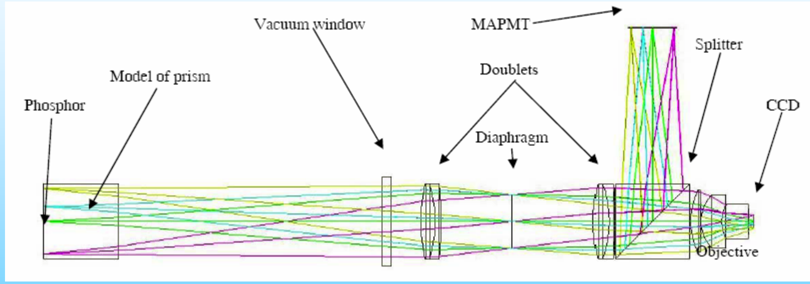

Ionization Profile Monitor

- Some (personal) remarks:
  - IMP still overestimates beam size

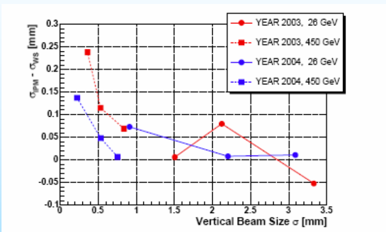

Figure 4: Comparison between IPM and WS derived from all the available measurements, in terms of beam size differences.

The Fig displays the absolute difference between the beam size measured by the IPM and the expected value at the IPM location derived from the Wire scanner measurements.

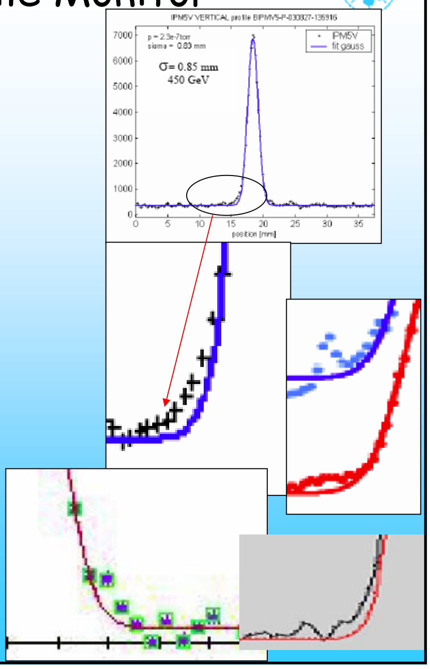

  - Resolution not better than 100 μm
  - Many Profiles show tails (artifacts?)
  - Dynamic range did not exceed 10^3.

Dynamic range did not exceed 10^3???

- CERN: Results of scraping vertically 1% of the distribution of a beam of $2.6 \cdot 10^{12}$ protons as seen by the IPM.

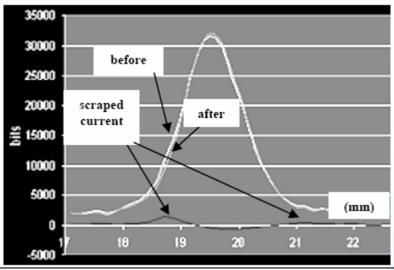

- J-Parc RCS: Idea to use additional MCP arrangement with lower resolution but high gain for halo observations.

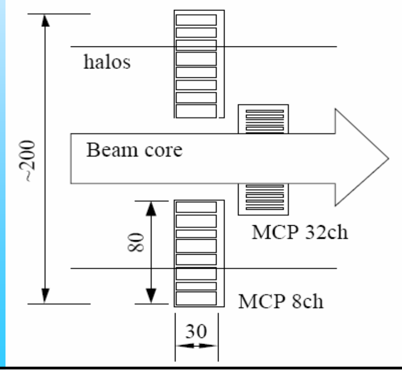

Luminescence Profile Monitor

(LPM)

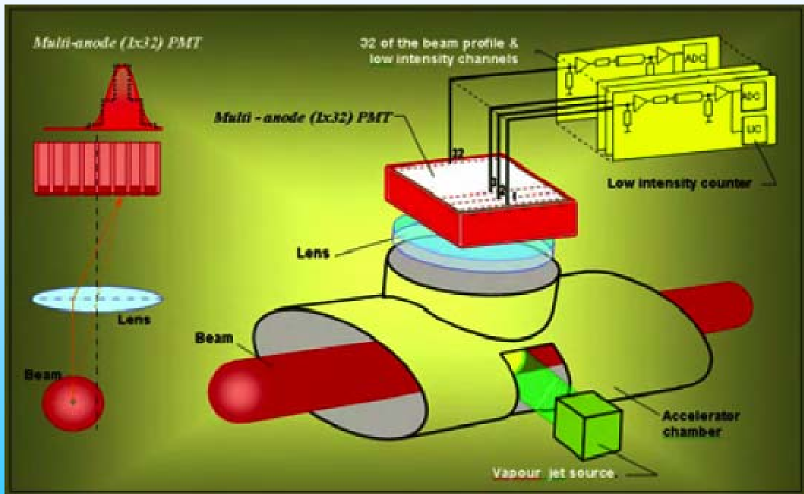

Luminescence Profile Monitor

- Gas Jet needed in most cases (H_2 or N_2)
- Sensitive muti anode PMT needed, therefore limited resolution (10^{-8} mbar).
- PEFP (Proton Engineering Frontier Project) use CCD camera at $4 \cdot 10^{-5}$ mbar
- Insensitive to electric and magnetic fields (space charge of beam, ext. fields)
- Limited dynamic range due to tails, high background and week signal
- COSY used shield against stray particles and light

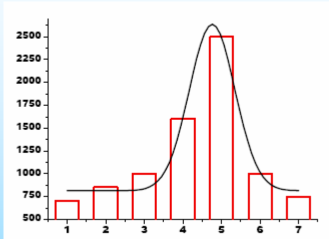

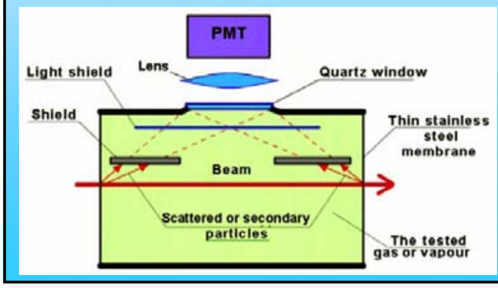

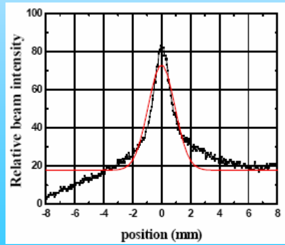

Luminescence Profile Monitor

I.P.H.I: We have to carry on additional experiments in order to understand more accurately the observed beam profiles… Huge background from several secondary processes. Try to discriminate background from real profile by Doppler shift of Balmer series.

Example: Ion source 100 keV, 100 mA protons
P. Ausset et al. (Orsay/Saclay)

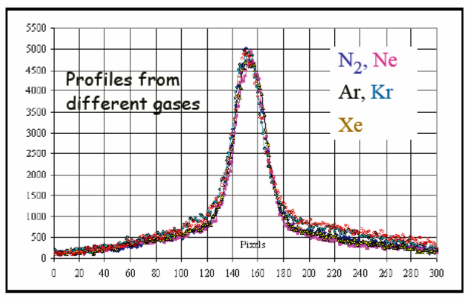

=> **Instrumental effects make it useless for Halo determination.**

Laser Profile Monitor

- Used for ions at SNS and J-PARC (beside electron beams (Compton))
  - H^- Beam photo neutralization
  - Collecting electrons
- SNS:
  - Profiles down to 3σ, dynamic range $\geq 10^3$

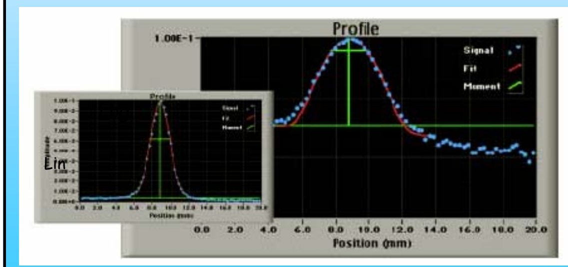

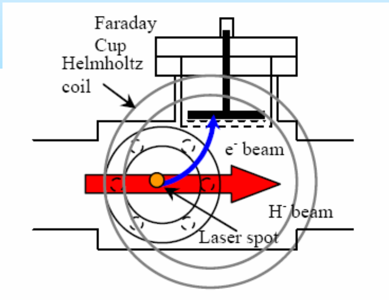

Laser Profile Monitor

- Halo Issue: Mechanical drift and vibration (SNS)
  - Compensation scheme foreseen, main frequencies up to 10 Hz